



# Study on the Capacity of Perforated Ferritic Stainless Steel Lipped Channel Columns

R. Dhanaiyendran<sup>(✉)</sup> and M. Anbarasu

Government college of Engineering, Salem, Tamilnadu, India  
dhanendran2108@gmail.com, gceanbu@gmail.com

**Abstract.** This work was primarily conducted to study the axial compression capacities of perforated ferritic stainless steel lipped channel compression members. Presently, there is reasonable demand for the application of cold-formed stainless steel in the building industry due to its improved material properties over cold-formed carbon steel, like improved corrosion resistance, durability, high strength-to-weight ratio, and also provides greater stiffness and recyclability leading to aesthetic appearance. Nickel content in the chemical compositions of ferritic stainless steel is low leads to achieve the cost-effectiveness over other types of stainless steel grades. Perforations in the web of the lipped channel column are used to cater to electrical wirings, plumbing lines, connection with other members and other building services. Perforations in the structural members also lead to lesser material consumption, which helps in reducing the dead load of the structure. Currently, limited studies are available on the performance of the cold-formed ferritic stainless steel lipped channel columns with web perforation. The numerical models were developed by using ABAQUS software and verified against the test results of cold-formed carbon steel perforated channel column sections subjected to axial compression. Validated numerical modelling approach was used to perform a parametric study by varying the cross-sectional geometries, global column slenderness and different perforation sizes. The strengths calculated from the parametric study were used to check the accuracy of the current codified Direct Strength Method (DSM) provisions in North American Standards (AISI S100:2016). Based on the results, the limitation of the current DSM codal provisions and the effect of perforation have been discussed.

**Keywords:** Cold-formed steel · Compressive strength · Direct Strength Method · Lipped channel · Stainless steel · Perforation

## 1 Introduction

Cold-formed stainless steel structural members have become promising building materials in aggressive environment of infrastructure construction mainly due to its improved material properties over cold-formed carbon steel, like high corrosion resistance, durability, high load carrying capacity to weight ratio and recyclability. Most stainless steels fall into one of three main classes- austenitic, martensitic and ferritic from their metallurgical structures. Low nickel content in the chemical compositions of ferritic stainless

steel leads to cost-effective construction over other types of stainless steel grades. Two different types of ferritic stainless steel in the AISI 400 series viz., SS 409 and SS 430. Stainless steel structural members are typically fabricated with perforations to ease various building services such as electrical and plumbing pipelines and wirings. However, the provision of hole in a structural member can affect the load transferring mechanism by causing stress redistribution within the structural member and cause the stress concentration around the holes, which leads to the regions vulnerable to failure. Different width to thickness ratio of perforation on various cross-sections shows noteworthy effects in the capacity of such columns. Currently, limited studies are reported on the assessment of structural performance of cold-formed stainless steel lipped channel columns with perforations.

Kulatunga and Macdonald (2013), investigated the introduction of perforations at alternate locations in the slender members, other than the column ends, which produced improved axial compressive strength. Local buckling was observed as the primary mode of failure in these specimens. Ashfan and Gardner (2013), conducted tests on ferritic stainless steel hollow columns and the results of which after comparing with the results of other grades of stainless steel with different shapes such as rectangular or square hollow columns from previously reported literature indicated that ferritic stainless steel offers promising structural performance at lower material cost. Umbarkar and Patton (2013), studied the influence of single circular hole in LDSS stub columns subjected to axial compressive load, the test results proves improved buckling resistance on increasing the thickness of the column member. And also the buckling load reduction was observed with the higher in the perforation size. Kulatunga and Macdonald (2014), studied the strength of cold-formed lipped channel compression member with perforations, imposed to axial compressive loading, concluded that increase in the perforation size (width to height ratio) shows dropping in the ultimate load. The results of the study carried out by Ye and Hajirasouliha (2018), showed that the maximum load capacities of the optimized CFS columns were on an average 20% more than the capacities of the commercially obtainable lipped channel columns. Singh and Singh (2018), investigated the conducting of cold-formed steel tubular stub columns with perforation, and their study displayed that the provision of perforation rises the local imperfection sizes of cold-formed steel hollow sections & compare to alternate perforation location, central perforation ratios up to 10% do not influence the ultimate capacity of such columns. Hence recommended to use a lesser perforation size. Degtyareva et al. (2020), investigated the local buckling capacity and design of cold-formed steel flexural member with slotted perforations, and concluded that the effect of staggered slotted perforations on local buckling capacity of the CFS flexural members is relatively very less, with a maximum decreased value of 11%. Chen et al. (2019), investigated cold -formed carbon steel channel columns having edges are stiffened and openings provided in web portion, the compression strength was more than the channel section without hole and also the channel section with stiffened edge with web openings provides promising results with the axial compressive strength of the channel section without hole.

From this literature survey it is found that there is no studies were reported on the perforated ferritic stainless steel lipped columns, and has been considered in the current research work. The main intent of this study is to examine the behavior and

axial strength of the perforated ferritic stainless steel lipped channel columns. The compressive strength of the perforated lipped columns is evaluated by using finite element analysis software ABAQUS. The validated finite element modelling procedure discussed in Sect. 2 is adopted for the parametric study. The strengths received from the parametric analysis were used to check the accuracy of the current codified DSM provisions in AISI Standards. Based on the analogy of results the limitation of the current codified DSM provisions and the impact of perforation on the strength of the members are discussed.

## 2 Finite- Element Modeling and Validation

The numerical models were evolved and validated versus the investigational test results of cold-formed carbon steel perforated channel sections imposed to axial compression (Chen et al. 2019). The FE modeling, validation are described subsequently in this sections.

### 2.1 Finite Element Modeling

The FEM analysis software ABAQUS was used to develop a non-linear numerical model to simulate the cold-formed steel perforated lipped columns subjected to direct axial compression loading.

The center line dimension of the cross section was used for numerical modeling. The perforations are made at the web face in the intermediate position at the mid-height of the member. The geometrical measurements and material properties of the cold-formed carbon steel channel section with perforations reported in literature (Chen et al. 2019) were used for the validation of the numerical modeling procedure. The element properties used for perforated ferritic stainless steel lipped channel sections were collected from (Rasmusan 2003). Conventional shell elements (S4R) were utilize to create model in perforated ferritic lipped channel columns. These elements permutate every node to have 3 DOF (degrees of freedom) both through the directions such as translation and rotation. Across the channel cross section (length & width), a mesh dimension of 5 mm  $\times$  5 mm was used for all perforated and plain lipped channel columns. The corner property is also assigned to the region of double times the member thickness (2 t) from the corners to enhance the ductility. Mesh refining was carried out around the perforation in web side.

Pinned boundary conditions were applied in all finite element models and the displacement and rotations to both ends were applied through middle (C.G) of the member cross section (Reference point). Two ends of the lipped columns were restrained by kinematic coupling available in ABAQUS through the reference points. To play the experimental boundary conditions, for reference point (1) at the top (loading point) the displacement in the two directions ( $x$  and  $y$ ) was constrained and vertical displacement in the ( $z$ ) direction was not constrained because of load is applied. The reference point (2) at the bottom (reaction point), the displacement in the all directions ( $x$ ,  $y$ ,  $z$ ) was restrained. Both ends of the column were unconfined to turn in minor axis, displacement control was provided at the loading point through axial load.

The global and local geometric imperfection sizes were included in the design according to their heights. The global imperfection amplitude was considered as  $L/1500$ , Where  $L$  = length of the specimen. The local imperfection amplitude for lipped channel columns were calculated formed on the equation was recommended by Dawson and Walker (1972). Two-step processes were carried for the validation of the simulated FE model. First, Subspace Eigen value available in the ABAQUS is used to extract the shortest buckling mode shape for the linear or elastic buckling examination and this extracted mode shape is used for the non-linear or plastic buckling analysis.

## 2.2 Validation Results

Using experimental tests done by (Chen et al. 2019) as reference, a set of finite element models were measured and confirmed. The finite element model used for modeling is presented here. Experimental results of all the 6 specimens are used to corroborate the efficiency of the finite element model in calculating axial capacities and the corresponding response of the experimental specimens. The results are conservative with each other with mean 1.03 and standard deviation 0.07 with reference to the table. Table 1 display the analogy of the experimental strengths ( $P_{Test}$ ) with numerical strength ( $P_{FEM}$ ) for channel columns with and without perforation. Figure 1 shows the comparison of deformed shape of finite element analysis with the experimental results.

**Table 1.** Validation of FEA results

Sl	Specimen ID	$P_{Test}$ (kN)	$P_{FEM}$ (kN)	$P_{Test}/P_{FEM}$ (kN)
1	<b>C190 × 45 × 15 × L750</b>	78.83	78.7	1.00
2	<b>C190 × 45 × 15 × L750-UHI</b>	60.62	59.59	1.01
3	<b>C240 × 45 × 15 × L-1500-UH3</b>	49.4	47.99	1.02
4	<b>C240 × 45 × 15 × L-1500-UH5</b>	49.37	46.41	1.06
5	<b>C190 × 45 × 15 × L1500-UH1</b>	46.87	49.25	0.95
6	<b>C190 × 45 × 15 × L-1500-NH0</b>	54.9	46.91	1.17
			Mean	1.03
			Standard deviation	0.07

\* NHO-Plain section, UH-Unstiffened web opening,  $P_{Test}$ –Ultimate load from experiments,  $P_{FEM}$ –Ultimate load from the FEM

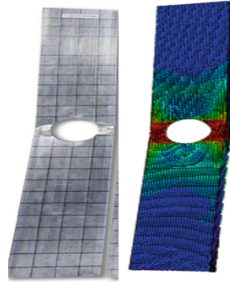


**Fig. 1.** C240 × 45 × 15 × L-1500-UH1.

### 3 Parametric Study

The confirmed FE or numerical models were applied to perform an ample parametric analysis by varying the geometric cross sections, global column slenderness and different perforation ratio. The perforation ratios were chosen in the range 0.1–0.5. Two different cross-sectional dimensions for this investigation were selected in accordance with the sizes obtainable from the optimized section reported in literature (Jun Yea and Iman Hajirasouliha 2018). A sum of 36 numerical models with column lengths different from 0.560–3.350 m were analysed as part of the recent work. The overall column slenderness (=0.25, 0.75, 1.5) was considered. Table 2 shows different sizes of specimens adopted in this analysis. Figure 2 shows the cross sectional view of the perforated lipped channel column.

**Table 2.** Different size of specimen for the study

Section	Channel depth $h$ (mm)	Channel width $b$ (mm)	Lip size $c$ (mm)	Specimen thickness $t$ (mm)	Corner radius (mm)
125 × 81 × 25	125	81	25	1.5	4
145 × 70 × 25	145	70	25	1.5	4

$h$  = channel depth (mm)

$b$  = channel width (mm)

$c$  = Lip size (mm)

$d/w$  = perforation ratio (0.1, 0.2, 0.3, 0.4, 0.5)

$L$  = length of the column

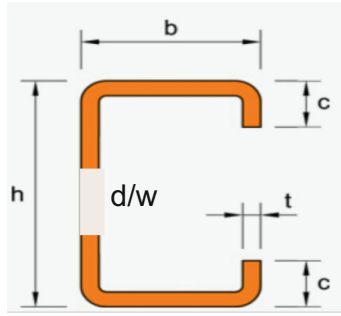


Fig. 2. Cross sectional view of perforated lipped channel column.

### 3.1 Parametric Study Results

The numerical investigation was performed for the different perforation ratio & heights for the selected specimens, and the results were noted. Table 3 Shows the peak load acquired by the FEM analysis for the parametric models considered in this study. Figure 3 shows deformed shape of  $125 \times 81 \times 25$  - L560 series varying perforation ratio (0, 0.1, 0.2, 0.3, 0.4 0.5). The plain column's concentration of stresses occur throughout the column while as in the perforated columns the concentration of stresses was observed around the perforations leading to local buckling. From Fig. 3 noted by Yielding failure at the vicinity of the perforation only, as represent by the deformed shape of the specimen. Figure 4 represents the load vs axial shortening curve generated from ABAQUS software for  $125 \times 81 \times 25$ -L560 series.

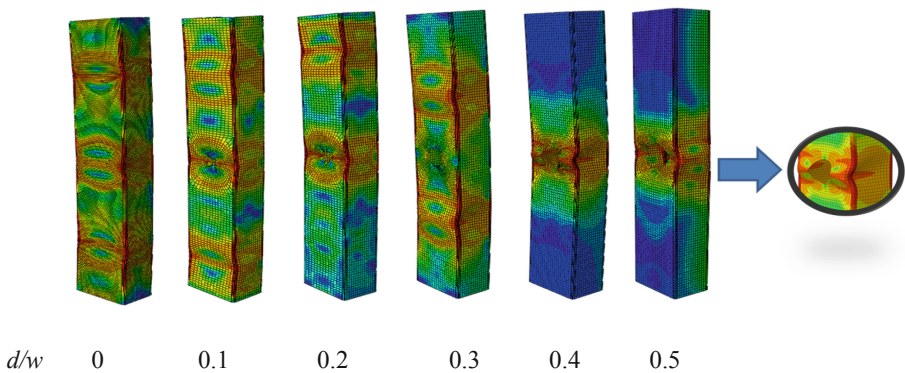


Fig. 3. Deformed shape of  $125 \times 81 \times 25$  -L560 series.

From Fig. 4, the ultimate load obtained from the curve without hole attains higher peak value when compared to perforated column with same length. With the increase in the flat to width ratio, a drop in the strength value is observed. The ultimate load in perforated column ( $d/w = 0.5$ ) is 13% lower when compared to the plain column of same dimensions. The axial shortening in perforated column ( $d/w = 0.5$ ) is 10% lower when compared to the plain column.

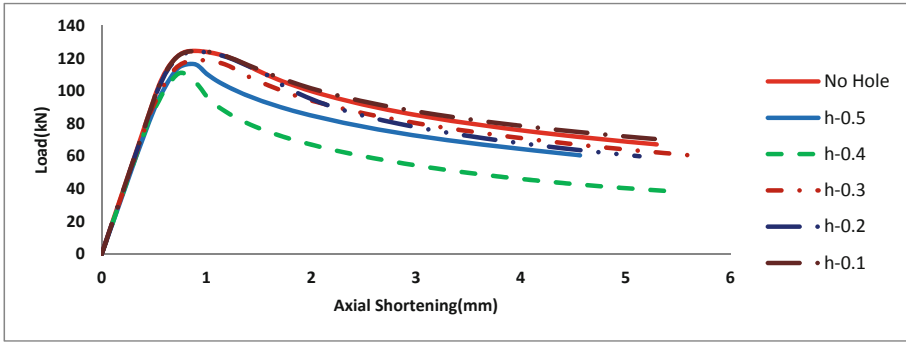


Fig. 4. Load vs axial shortening curve.

### 4 Direct Strength Method

This method is most suitable to predict the capacity of thin walled structural members. The elastic properties of a general thin walled steel members are obtained from an elastic buckling curve. The buckling curve was created by utilize the finite strip technique (CUFSM). The elastic buckling strength of the member with perforation was determined evolved from equations suggested by Yu and Schafer. The axial compression capacity of the lipped channel column was evaluated centred on the design calculations provided in North American standards AISI S100–2016. In this study, the suitability of design equations for lipped channel columns with perforation at the center of the member using DSM is assessed. Strength of the perforated column is evaluated as per DSM based upon three checks viz, global buckling failure ( $P_{ne}$ ), local buckling failure ( $P_{nl}$ ), and distortional buckling failure ( $P_{nd}$ ). The buckling resistance of the compression member is the least of ( $P_{ne}$ ,  $P_{nd}$ ,  $P_{nl}$ ). Table 3 presents the comparison of compression capacities with varying length and perforation ratios with two different cross sections.

Table 3. Comparison of results

Sl	Section ID (mm)	Ultimate load $P_{FEM}$ (kN)	Ultimate load $P_{DSM}$ (kN)	$P_{FEM}/P_{DSM}$
1	125 × 81 × 25–560-0	124.44	120.75	1.03
2	125 × 81 × 25–560-0.1	124.43	113.19	1.10
3	125 × 81 × 25–560-0.2	123.85	119.44	1.04
4	125 × 81 × 25–560-0.3	118.9	120.61	0.99

(continued)

**Table 3.** (continued)

Sl	Section ID (mm)	Ultimate load $P_{FEM}$ (kN)	Ultimate load $P_{DSM}$ (kN)	$P_{FEM}/P_{DSM}$
5	<b>125 × 81 × 25-560-0.4</b>	111.12	115.62	0.96
6	<b>125 × 81 × 25-560-0.5</b>	116.23	114.27	1.02
7	<b>125 × 81 × 25-1680-0</b>	107.04	107	1.00
8	<b>125 × 81 × 25-1680-0.1</b>	105.12	101.42	1.04
9	<b>125 × 81 × 25-1680-0.2</b>	107.41	105.78	1.02
10	<b>125 × 81 × 25-1680-0.3</b>	103.72	113.47	0.91
11	<b>125 × 81 × 25-1680-0.4</b>	102.23	105.32	0.97
12	<b>125 × 81 × 25-1680-0.5</b>	101.22	101.70	1.00
13	<b>125 × 81 × 25-3350-0</b>	80.01	73.57	1.09
14	<b>125 × 81 × 25-3350-0.1</b>	79.008	67.135	1.18
15	<b>125 × 81 × 25-3350-0.2</b>	78.725	70.392	1.12
16	<b>125 × 81 × 25-3350-0.3</b>	76.418	70.019	1.09
17	<b>125 × 81 × 25-3350-0.4</b>	73.944	75.188	0.98
18	<b>125 × 81 × 25-3350-0.5</b>	72.57	74.328	0.98
19	<b>145 × 70 × 25-490-0</b>	130.38	110	1.19
20	<b>145 × 70 × 25-490-0.1</b>	120.68	102.68	1.18

(continued)



**Table 3.** (continued)

Sl	Section ID (mm)	Ultimate load $P_{FEM}$ (kN)	Ultimate load $P_{DSM}$ (kN)	$P_{FEM}/P_{DSM}$
21	<b>145 × 70 × 25-490-0.2</b>	144.54	108.81	1.33
22	<b>145 × 70 × 25-490-0.3</b>	119.12	112.99	1.05
23	<b>145 × 70 × 25-490-0.4</b>	106.37	110.2	0.97
24	<b>145 × 70 × 25-490-0.5</b>	107.13	102.61	1.04
25	<b>145 × 70 × 25-1450-0</b>	103.35	103	1.00
26	<b>145 × 70 × 25-1450-0.1</b>	98.456	95.799	1.03
27	<b>145 × 70 × 25-1450-0.2</b>	90.005	102.72	0.88
28	<b>145 × 70 × 25-1450-0.3</b>	95.927	108.77	0.88
29	<b>145 × 70 × 25-1450-0.4</b>	96.302	102.4	0.94
30	<b>145 × 70 × 25-1450-0.5</b>	94.218	95.193	0.99
31	<b>145 × 70 × 25-2930-0</b>	63.292	81	0.78
32	<b>145 × 70 × 25-2930-0.1</b>	72.263	75.33	0.96
33	<b>145 × 70 × 25-2930-0.2</b>	67.533	75.118	0.90
34	<b>145 × 70 × 25-2930-0.3</b>	66.58	75.27	0.88
35	<b>145 × 70 × 25-2930-0.4</b>	68.132	75.181	0.91
36	<b>145 × 70 × 25-2930-0.5</b>	60.077	73.39	0.82
			Mean	1.01
			Standard deviation	0.10

Local buckling is observed as the primary mode of failure in these all specimens. The buckling failure occurring all the specimens is initiated by the presence of perforation. From the Table 3 noted by varying the cross sectional geometrics, global column slenderness and different perforation sizes, the axial strength of perforated columns dropped when increasing the perforation size. Further the compressive strength of the column member decreases with an increase the slenderness of column. The specimen have equal cross sectional area with different slenderness and perforation sizes increase in the order (0.1–0.5), the model with least perforation is able to carry peak load at minimum rate of strain or deformation.

## 5 Conclusion

This research work described the study on the axial compression strengths of the perforated ferritic stainless steel lipped channel columns. The numerical model was developed by using the numerical analysis software ABAQUS [6.13] and the results are checked versus the experimental results of cold-formed carbon steel perforated columns subjected to axial compressive strength. The section are selected hinged on the optimized sections reported in literature are considered for the parametric study. The verified numerical model procedure is used to perform the parametric analysis. Finally the axial compression strength of perforated columns obtained from the parametric study is compared with the predictions of the current codified Direct strength Method provisions in North American Standards (AISI S 100:2016). The known results are following from this study are given below.

1. The axial strength of the perforated ferritic lipped channel columns dropped when increasing width to depth ( $d/w$ ) ratio.
2. It is noted that the members exhibit yielding failure at the vicinity of the perforation only, as indicated by the deformed shape of the section.
3. The compressive strength of the plain ferritic lipped columns (without hole) decreases with an increase the length of the column.
4. The plain column's concentration of stresses occur throughout the column while as in perforated column the concentration of stresses around the hole leads to local buckling.
5. The ultimate load in perforated column ( $d/w = 0.5$ ) is 13% less as compared to the plain column. The axial shortening of perforated column ( $d/w = 0.5$ ) is 10% lower than that of the plain column.
6. Local buckling is perceived as the primary mode of failure in these all specimens.
7. If the models have equal cross sectional area with varying heights and perforation ratios increase in the order of (0.1–0.5), the model with lowest perforation (0.1) is able to carry maximum load at minimum rate of deformation.

## References

- Ashfan, S., Gardner, L.: Experimental study on cold-formed ferritic stainless hollow sections. *J. Struct. Eng.* **139**, 717–728 (2013)

- Anbarasu, M., Ashraf, M.: Behavior and design of cold-formed lean duplex stainless steel lipped channel columns. *Thin Walled Struct.* **104**, 106–115 (2016)
- Arrayago, I., Mirambell, E.: Experimental study on ferritic stainless RHS and SHS beam-column. *Thin Walled Struct.* **100**, 93–104 (2016)
- Anbarasu, M., Ashraf, M.: Interaction of local flexural buckling for lean duplex stainless steel hollow columns. *Thin Walled Struct.* **112**, 20–30 (2017)
- Chen, B., et al.: Effects of edge-stiffened web openings on the behaviour of cold-formed steel channel sections under compression. *Thin-Walled Struct.* **144**, 106307 (2019)
- Dawson, R., Walker, A.C.: Post buckling of geometrically imperfect plates. *J. Struct. Div.* **98**, 75–94 (1972)
- Ellobody, E., Young, B.: Structural performance of cold-formed high strength stainless steel columns. *J. Constr. Steel Res.* **61**, 1631–1649 (2005)
- Yea, J., Hajirasouliha, I.: Experimental investigation of local-flexural interactive buckling of cold formed steel channel columns. *Thin-Wall Struct.* **125**, 245–258 (2018)
- Kulatunga, M.P., Macdonald, M.: Investigation of cold-formed steel structural members with perforations of different arrangements subjected to compression loading. *Thin Walled Struct.* **67**, 78–87 (2013)
- Liu, Y., Young, B.: Buckling of stainless steel square hollow section compression members. *J. Constr. Steel Res.* **59**(2), 165–177 (2010)
- Degtyareva, N., Gatheeshgar, P., Poologanathan, K., Gunalan, S., Shyha, I., McIntosh, A.: Local buckling strength and design of cold-formed steel beams with slotted perforations. *Thin-Walled Struct.* **156**, 106951 (2020). <https://doi.org/10.1016/j.tws.2020.106951>
- Rasmusan, K.J.R.: Full-range stress strain curves for stainless steel alloys. *J. Constr. Steel* **59**, 47–61 (2003)
- Singh, T.G., Singh, K.D.: Experimental investigation on performance of perforated cold-formed steel tubular stub columns. *Thin-Walled Struct.* **137**, 107–121 (2018)